MODE II FATIGUE CRACK GROWTH CHARACTERISTICS AND MECHANISM IN ALUMINUM ALLOY 7N01-T4 WELDMENTS UNDER MODE II LOADING

A. Otsuka, K. Tohgo, T. Kiba[1] and S. Yamada[2]

Department of Iron & Steel Engineering, Nagoya University Nagoya 464, Japan

ABSTRACT

Mode II fatigue crack growth behavior has been investigated on 7N01-T4 aluminum alloy weldments by four-point shear loading. da/dN-ΔK_{II} relations and ΔK_{II}-threshold for mode II fatigue crack growth have been obtained for base metal-, HAZ-, and weld metal-specimens. HAZ-specimens showed very low ΔK_{IIth} for mode II growth ($\approx$ 1MPa$\cdot\sqrt{m}$), compared with those of base metal- and weld metal-specimens (9-10MPa$\cdot\sqrt{m}$). Based on the observations of the deformation near the crack tip at the successive stages of a loading cycle (namely at K_{min}, K_{max} and K_{min}), a mechanism of mode II fatigue crack growth has been proposed.

KEYWORDS

Mode II fatigue crack growth; ΔK_{II}-threshold; Mechanism of fatigue; BCS model; Aluminum alloy; Fractograph; Four-point shear loading test.

INTRODUCTION

Fatigue behavior under cyclic mode II loading has been investigated by several authors (Roberts and Kibler, 1971; Pook, 1977; Yokobori, Yokobori, and Kamei, 1977) using various loading techniques. Our previous investigations (Otsuka and others, 1980, 1981a, 1981b; Otsuka, Mori, and Tokumasu, 1982; Otsuka and Mori, 1983) on mode II fatigue crack growth of aluminum alloys and mild steel were made by a specially designed apparatus. The results obtained by our previous tests, however, were limited to the small-sized thin base metal specimens because of the limitation of the test apparatus. In the present work, tests were made on thicker specimens of welded parts by using the four-point shear loading test technique. The

1 Present affiliation : Yokohama Metal Works, Metal Products Division, Toshiba Corporation, Shinsugitacho, Isogoku, Yokohama 235, Japan
2 Present affiliation : Rinnai Corporation, Fukuzumi-cho, Nakagawa-ku, Nagoya 454, Japan

TABLE 1 Chemical composition(%) and mechanical properties

	Cu	Si	Fe	Mn	Mg	Zn	Cr	Ti	Zr	Al	Yield Stress (MPa)	U.T.S (MPa)	Elongation (%)
7N01-T4	0.13	0.09	0.19	0.34	1.35	4.33	0.12	0.06	0.14	Re	294	345	20.0
Wire,A5556WY	0.01	0.07	0.17	0.63	5.00	0.02	0.09	0.09	-	Re	133	283	14.7

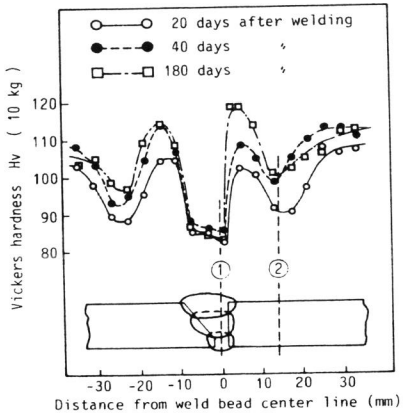

Fig. 1 Vickers hardness of 7N01-T4 weld. ① and ② show the locations of slits of weld metal-, and HAZ-specimens, respectively.

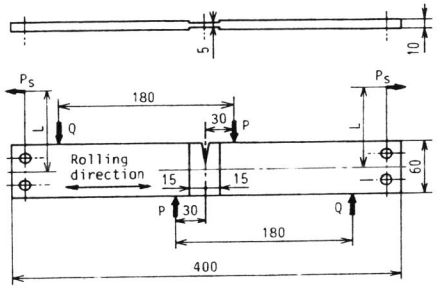

Fig. 2 Four-point shear specimen. Dimensions are shown in mm.

advantage of this method will be in its applicability to larger specimens with various geometries such as welded connections. Another advantage of this method is good accessibility to the specimen surface, which enabled close examination of the specimens. Based on the observation of the deformation behavior near the crack tip, a mechanism of mode II fatigue crack growth is proposed.

MATERIALS AND EXPERIMENTAL PROCEDURE

Tests were made on base metal, HAZ, and weld metal of 7N01-T4 aluminum alloy. The chemical composition and mechanical properties of the aluminum alloy and the electrode wire are shown in Table 1. The Vickers hardness number of the welded part is shown in Fig. 1. Fatigue tests were made on base metal-, HAZ-, and weld metal-specimens, by using the specimens shown in Fig. 2. The positions of the slits in HAZ-specimens and weld metal-specimens are shown in Fig. 1.

Mode II fatigue tests have been carried out under the conditions of cyclic mode II loading ΔK_{II} superimposed by static K_I, K_{IS}. ΔK_{II} was given by four-point shear loading and K_{IS} was given by load P_s, as shown in Fig. 2. da/dN-ΔK_{II} relations and ΔK_{II}-threshold for mode II fatigue crack growth were obtained by ΔK_{II}-increasing and ΔK_{II}-decreasing tests at the stress ratio R = 0.05. Tests were carried out in air by an electro-hydraulic servo fatigue testing machine at the frequency of 3-10Hz.

In order to investigate the process of mode II fatigue crack growth, the

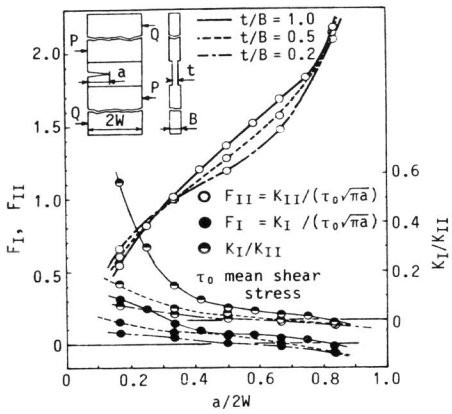

Fig. 3 K_I and K_{II} values of side-notched specimen under four-point shear loading.

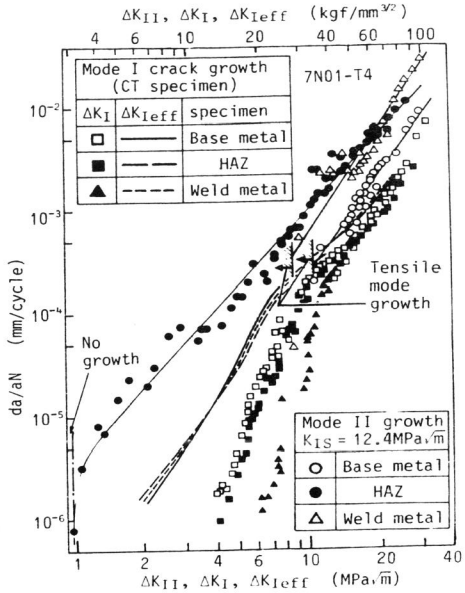

Fig. 4 da/dN(mode II growth)-ΔK_{II}, da/dN(mode I growth)-ΔK_I, and da/dN(mode I growth)-ΔK_{Ieff} relations for base metal-, HAZ-, and weld metal-specimens, where $\Delta K_{Ieff} = K_{Imax} - K_{Iop}$.

deformation field near the crack tip under cyclic mode II loading was measured by the lines scribed on the specimen surface. The parallel lines as shown in Fig. 6 were scribed on the specimen surface, before the test, by emery paper in the direction normal to the crack. During the test, plastic replicas of the crack tip were taken at some selected ΔK_{II} values to observe the variation of the deformation state during load cycles. The replicas were taken at the successive points of K_{IImin}, K_{IImax}, and K_{IImin}, as shown in Fig. 6.

The stress intensity factors K_I and K_{II} of edge-cracked specimens under four-point shear loading were calculated by a finite element method with isoparametric quadrilateral elements. The details of the analysis were reported in another papers (Otsuka and others, 1982; Otsuka, Tohgo and Yamada, 1983). The results are given in Fig. 3 for three cases, t/B = 0.2, 0.5 and 1.0, where B is the specimen thickness and t is the thickness of the central thinned part of the specimen as shown in Fig. 2. F_I and F_{II} in Fig. 3 are defined by $F_I = \frac{K_I}{\tau_0\sqrt{\pi a}}$, $F_{II} = \frac{K_{II}}{\tau_0\sqrt{\pi a}}$, and τ_0 is given by $\tau_0 = \frac{P-Q}{2Wt}$. According to the result of Fig. 3, it is seen that if a/2W>0.3 and t/B<0.5, K_I/K_{II}<0.1. The present tests were carried out under the conditions which satisfy these requirements.

RESULTS AND DISCUSSION

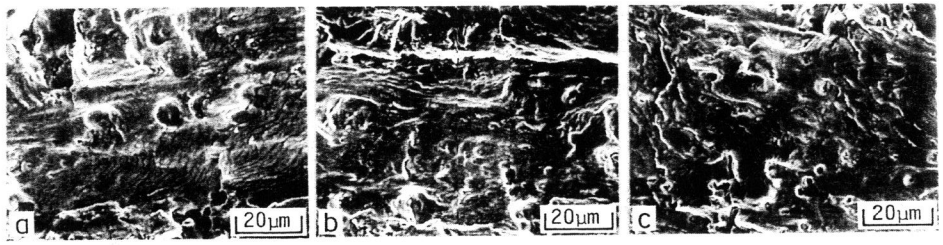

Fig. 5 Fractographs of mode II fatigue crack growth in 7N01-T4.
(a)Base metal, ΔK_{II}=18 MPa$\sqrt{m}$.(b)HAZ, ΔK_{II}=20 MPa$\sqrt{m}$.(c)Weld metal, ΔK_{II}=13 MPa$\sqrt{m}$.
Macroscopic direction of fatigue crack growth is from left to right.

Four-point Shear Loading Test

The accuracy and reliability of this four-point shear method were confirmed by comparing the test results with those reported in the previous papers (Otsuka and others, 1980, 1981a, 1981b). In either case, tests were made on 2017-T4 and 7075-T6 aluminum alloys, and it was confirmed that the results obtained by both methods agree quite well (Otsuka, Tohgo and Yamada, 1983). It was concluded from these results that the accuracy and reliability of both methods for mode II fatigue crack growth, namely, four point shear method and previous one are quite satisfactory. As already shown in the previous papers (Otsuka and others, 1980, 1981a, 1981b), K_{IS} actually has no effect on mode II growth, as long as a K_{IS} of enough magnitude to prevent rubbing action between the mating fracture surfaces is applied.

Mode II Fatigue Crack Growth Behavior in 7N01-T4 Aluminum Alloy Weldment

Fig. 4 shows the da/dN for mode II fatigue crack growth versus ΔK_{II} relation for base metal-, HAZ-, and weld metal-specimens of 7N01-T4 aluminum alloy obtained by four-point shear method. For comparison, usual da/dN-ΔK_I and da/dN-ΔK_{Ieff} relation for mode I loading obtained by 5mm thick 1CT specimen are also shown for these specimens. It is noticed firstly that the HAZ-specimens show very low ΔK_{II}-threshold for mode II growth ($\approx$ 1MPa$\cdot\sqrt{m}$), compared with those of base metal- and weld metal-specimens (9-10MPa$\cdot\sqrt{m}$). It is most interesting to notice that this low resistance of HAZ-specimen for fatigue crack growth is seen only for mode II growth and not for mode I growth, namely, base metal-, HAZ-, and weld metal-specimens show almost the same mode I fatigue crack growth behavior under mode I loading, as shown in the da/dN-ΔK_{Ieff} relation in Fig. 4. Here, some explanations on the definitions of the ΔK_{IIth}-threshold for mode II growth, ΔK_{IIth}(mode II growth), should be made. In base metal- and weld metal-specimens, the ΔK_{IIth}(mode II growth) indicates, as shown in Fig. 4, ΔK_{II} level at which the transition from mode II growth to mode I growth occurs, whereas for the HAZ-specimens, the ΔK_{IIth}(mode II growth) indicates the ΔK_{II} level, where the mode II crack is arrested. Thus in the base metal and weld metal, mode I growth occurs below the ΔK_{IIth}(mode II growth) levels, while in HAZ below the ΔK_{IIth}(mode II growth) level, no fatigue crack growth occurs.

Though the material dependence of da/dN for mode II growth does not seems to be as large as that of ΔK_{IIth}(mode II growth), HAZ- and weld metal-specimens show higher mode II growth rate than base metal-specimens do by a factor of 3 or 4. As noticed in the previous report on 2017-T4 and 7075-T6, da/dN for mode II growth shows, in 7N01-T4, too, higher value than da/dN for mode I

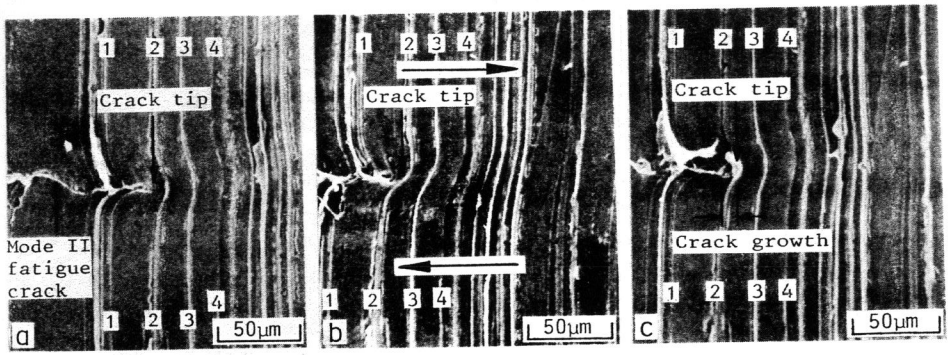

Fig. 6 Observations of mode II fatigue crack growth during one load cycle in HAZ. Lines scribed on the specimen surface by emery paper show the deformation around the crack. (a) at the minimum load, K_{II}=1.12 MPa$\sqrt{m}$. (b) at the maximum load, K_{II}=22.4 MPa$\sqrt{m}$. (c) at the minimum load, K_{II}=1.12 MPa$\sqrt{m}$. Arrows in Fig.(b) show the direction of shearing stress.

growth by a factor of 5-7, if they are compared at $\Delta K_I = \Delta K_{II}$. Figures 5(a), (b), and (c) show the fractographs of base metal-, HAZ-, and weld metal-specimens, respectively. Though some differences exist among them, it seems to be rather reasonable to assume that there is no essential differences among the fractographs of base metal-, HAZ-, and weld metal-specimens, because such differences observable in these figures are not unusual in the same specimen according to the field of view. Striation-like patterns and dimples in Figs. 5(a) and (c), respectively, may be assumed to be incidental and to have no meaningful correlation with the mechanism of mode II growth, because mode II growth does occur without them as seen, for instance, in Figs. 8(a) and (c).

Mechanism of Mode II Fatigue Crack Growth

Figure 6 shows the deformation around the crack tip under mode II cyclic loading in a HAZ-specimen. Figures (a), (b), and (c) show the appearance at the successive stages - minimum load, maximum load, minimum load - in one loading cycle. These SEM photographs are those of replicas taken at each stage of the loading. Based on the results shown in Fig. 6, the process of mode II fatigue crack growth is illustrated schematically in Fig. 7, where Figs. (a), (b), and (c) correspond to Figs. 6(a), (b), and (c), respectively.

At the maximum load, new surface AB is created on the lower fracture surface by slip occurred at the crack tip as shown in Fig. 7(b). In the process of unloading, new surface A'B' is formed on the upper surface in the similar way to AB, due to the reversed shear displacement caused by the elastic unloading of the surrounding material. Fatigue crack growth in one cycle is almost equal to this crack tip shear displacement on the crack surface as will be seen from Fig. 6. We call this amount "Crack Tip Shear Displacement on crack surface" $\Delta(CTSD)_c$. We measured another quantity $\Delta(CTSD)_p$ "Crack Tip Shear Displacement on the boundary of plastic zone", as shown in Fig. 7. As seen in Fig. 6, severe plastic deformation is observed along and ahead the crack, and in the region outside of this heavily deformed plastic region, the reference lines scribed by the emery paper are almost straight. $\Delta(CTSD)_p$ was determined as the value of the shear displacement of these lines behind the crack tip extrapolated to the crack tip. The plastic zone defined here will

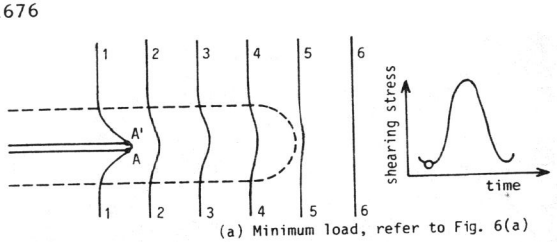

(a) Minimum load, refer to Fig. 6(a)

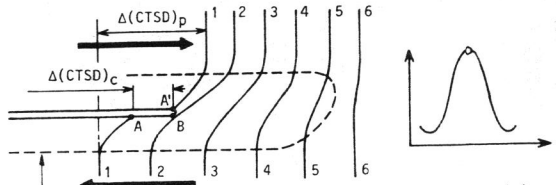

(b) Maximum load, refer to Fig. 6(b)

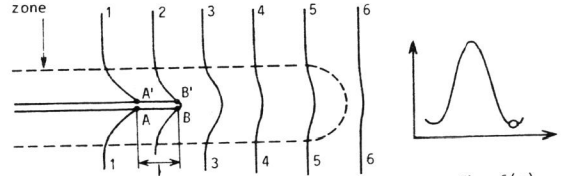

Fatigue crack growth in one load cycle

(c) Minimum load, refer to Fig. 6(c)

Fig. 7 Schematic illustration of the process of mode II fatigue crack growth. (a) at the minimum load. (b) at the maximum load. (c) at the minimum load.

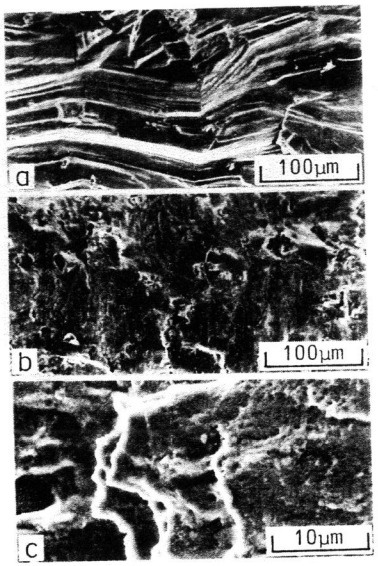

Fig. 8 Typical examples of fractograhps of mode II fatigue crack growth. (a)2017-T4,Extruded bar,ΔK_{II}=1.7MPa$\sqrt{m}$. (b)2017-T4,Extruded bar,ΔK_{II}=20.3MPa$\sqrt{m}$. (c)7075-T6,Rolled plate,ΔK_{II}=7.1MPa$\sqrt{m}$.

essentially correspond to cyclic plastic zone, though more investigation is needed on the behavior of this zone. $\Delta(CTSD)_p$ has the meaning of the integration of the shear strain in the plastic zone ahead of the crack. $\Delta(CTSD)_p$ obtained at various values of ΔK_{II} are shown in Fig. 9, along with the da/dN obtained from the crack length measured by a travelling microscope and shear displacement by BCS theory (Bilby, Cottrell and Swinden, 1963) $\Phi(a)$ obtained by the following formula.

$$\Phi(a) = \frac{8(1-\nu^2)\tau_{ys}^c\, a}{\pi E}\log\{\sec(\frac{\pi}{2}\frac{\Delta\tau}{\tau_{ys}^c})\} \approx \frac{(1-\nu^2)\,\Delta K_{II}^2}{E\tau_{ys}^c}, \qquad \frac{\Delta\tau}{\tau_{ys}^c} << 1 \quad . \quad (1)$$

where a = crack length, $\Delta\tau$ = range of applied shear stress,
ΔK_{II} ($= \Delta\tau\sqrt{\pi a}$) = range of K_{II},
τ_{ys}^c = cyclic yielding shear stress,
ν = Poisson's ratio, and E = Young's modulus.

The following values were used for the calculation.
$\tau_{ys}^c = 2\tau_{ys}$ = 340MPa, E = 76000MPa, and ν = 0.3
From Fig. 9 the following characteristics are observed.
(1) $\Delta(CTSD)_p$ is almost equal for base metal-, HAZ- and weld metal-specimens, and it agrees quite well with the value obtained from BCS theory, in this aluminum alloy.
(2) The ratios of da/dN to $\Delta(CTSD)_p$ are 1/10-1/4 for base metal, and 1/3-

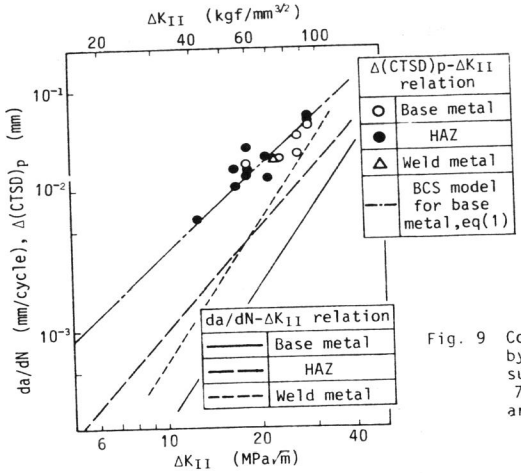

Fig. 9 Comparison of $\Delta(CTSD)_p$ obtained by the observation of specimen surface in the way shown in Fig. 7 with $\Delta(CTSD)_p$ by BCS theory and da/dN

1/2 for HAZ and weld metal. At higher ΔK_{II} the difference between da/dN and $\Delta(CTSD)_p$ is smaller. The result (1) seems to be reasonable if we assume that the shear displacement given by BCS theory is distributed in the plastic region as shown in Fig. 7. For result (2), the differences among the $(da/dN)/\Delta(CTSD)_p$'s, the values is almost equal to the $\Delta(CTSD)_c/\Delta(CTSD)_p$'s, of base metal, HAZ and weld metal are due to the difference in their plastic deformation behavior. From practical view point, da/dN for mode II growth will be estimated by assuming appropriate values of the ratio $\Delta(CTSD)_c/\Delta(CTSD)_p$, if the $\Delta(CTSD)_p$ can be obtained from BCS theory with good accuracy as in this case, though further work is needed to confirm this relation.

Though the dependence of fractographs of mode II fatigue crack growth on the magnitude of ΔK_{II} is not always clear (for instance, in 7075-T6 and 7N01-T4), in some cases the dependence is very clear as shown in Figs. 8(a) and (b). In such cases, the fracture surface is usually crystallographic at low ΔK_{II} as shown in Fig. 8(a), while at higher ΔK_{II} it shows non-crystallographic rather smooth appearance, as shown in Fig. 8(b), which seems to be formed by shear decohesion. Another feature, the topography described as "shearing a pack of cards", as shown in Fig. 8(c), is sometimes observed. This topography can be explained by assuming that slip displacement occurs in several planes simultaneously. It is also interesting to notice that the direction of fatigue crack growth is towards the leading edges of the layers for both upper and lower fracture surfaces of mating surfaces; i.e. from left to right in Fig. 8(c). These features, shown in Figs. 8(a) ~ (c), seem to support the idea, which is shown in Fig. 7, that mode II growth is the direct result of slip or shear displacement.

CONCLUSIONS

1. The accuracy and applicability of four-point shear loading test as a mode II fatigue crack growth test have been confirmed by the tests on aluminum alloys 2017-T4, 7075-T6, and 7N01-T4 weldments.
2. According to the test results on 7N01-T4 weldments, HAZ-specimens show very low ΔK_{IIth}(for mode II growth), compared with base metal- and weld

metal-specimens, though essentially no difference is found between the mode I fatigue crack growth characteristics of these specimens. This difference in behavior between mode I growth and mode II growth comes from their difference in the mechanism of fatigue crack growth.

3. Based on the observations of the deformation near the crack tip during the loading cycle, a mechanism of mode II fatigue crack growth has been proposed.

ACKNOWLEDGEMENT

The authors wish to thank Messrs. C. E. Skjølstrup and K. Sakakibara, graduate students of Nagoya University, for their assistance in experiments.

REFERENCES

Bilby, B. A., A. H. Cottrell, and K. H. Swinden (1963). The spread of plastic yield from a notch, Proc. Roy. Soc., A, 272, 304-314.

Otsuka, A., K. Mori, T. Ohshima, and S. Tsuyama (1980). Fatigue crack growth of steel and aluminum alloy specimens under mode II loading, J. Soc. Materials Science, Japan, 29, 1042-1048. (in Japanese)

Otsuka, A., K. Mori, S. Tsuyama, and Y. Sumiya (1981). In G. C. Sih and M. Mirable (Eds.), Analytical and Experimental Fracture Mechanics, Sijthoff & Noordhoff, The Netherland. pp.375-386.

Otsuka, A., K. Mori, T. Ohshima and T. Sumiya (1981). In D. Francois, et al. (Eds.), Advances in Fracture Research, vol.4, Pergamon, Oxford. pp.1851-1858.

Otsuka, A., K. Mori, and H. Tokumasu (1982). Initiation of mode II fatigue crack growth from fatigue precrack and machined slit in aluminum alloys, J. Soc. Materials Science, Japan, 31, 662-668. (in Japanese)

Otsuka, A., T. Miyata, K. Tohgo, S. Yamada and T. Kiba (1982). An investigation on Mode II fatigue crack growth of aluminum alloy weldments by four-point shear loading method, preprint of the 16th Symposium on Fatigue, Soc. Materials Science, Japan, 26-30. (in Japanese)

Otsuka, A., and K. Mori (1983). Fractographic study of mode II fatigue crack growth on 7075-T6 and 2017-T4 aluminum alloys, J. Soc. Materials Science, Japan, 32, 282-388. (in Japanese)

Otsuka, A., K. Tohgo, and S. Yamada (1983), Mode II fatigue characteristics of 7N01-T4 Weldments, Preprint of the Japan Soc. Mech. Eng., No.830-10, 219-221. (in Japanese)

Pook, L. P. (1977). An observation on mode II fatigue crack growth threshold behavior, Int. J. of Fracture, 13, 867-869.

Roberts, R. and J. J. Kibler (1971). Mode II fatigue crack propagation, Trans. ASME, Series D, 93, 671-680.

Yokobori, T., A. T. Yokobori, and A. Kamei (1977). Fatigue crack growth under mode II loading, Trans. Japan Soc. Mech. Engineers, 43, 4345-4352. (in Japanese)